Journal of the Serbian Society for Computational Mechanics / Vol. 11 / No.1, 2017 / pp. 59-68
(DOI: 10.24874/jsscm.2017.11.01.06)

A Detailed Study of Effects of Row Trenched Holes at the Combustor Exit on Film Cooling Effectiveness

E. Kianpour[1*] and N. A. Che Sidik[2]

[1] Department of Mechanical Engineering, Najafabad Branch, Islamic Azad University, Najafabad, Iran
e-mail: ekianpour@pmc.iaun.ac.ir
[2] Department of Thermo-fluid, Faculty of Mechanical Engineering, University Technology of Malaysia, Skudai, Johor, Malaysia
e-mail: azwadi@utm.my
**corresponding author*

Abstract

The current research was performed in order to analyze the effects of cylindrical and row trench cooling holes with the alignment angle of 90 degrees on the film-cooling effectiveness near the combustor endwall surface at the blowing ratio of BR=3.18. The three-dimensional representation of a Pratt and Whitney gas turbine engine was simulated and analyzed with the commercial finite volume package, FLUENT 6.2.26. in order to find the most effective row trenched cooling holes. The analysis was done with Reynolds averaged Navier–Stokes turbulence model (RANS) on internal cooling passages. This combustor simulator was combined with the interaction of two rows of dilution jets, which were staggered in the stream-wise direction and aligned in the spanwise direction. In comparison with the baseline case of cooling holes, using a row trenched hole near the endwall surface increased the film-cooling effectiveness by 44% in average.

Keywords: Gas turbine engine, film-cooling, trench hole, dilution hole

1. Introduction

Advanced gas turbine industries try to extend the gas turbine engine efficiencies. Brayton cycle is a key to achieve this purpose. In this cycle, in order to have higher gas turbine engine efficiency, the combustor's outlet temperature must increase (Salimi et al. 2014). However, such hot flows cause non-uniformities at the end of the combustor and at the inlet of the turbine and damage the critical parts. Film cooling is the most well-known method of preservation. In this technique, a low temperature thin layer attaches to a surface and protects it against hot streams. To get better film cooling performance, it is needed to increase the blowing ratio. The blowing ratio increment has an intense effect on the heat transfer, particularly in the hole region. According to the importance of this study, a broad literature survey was done to get the fundamental data.

Researchers analyzed the effects of hole angle geometries on film cooling (Abdullah et al. 2012). They considered four different rows of inclined holes with angles of 20 degrees and 35

degrees. They made ready the contours which showed the laterally averaged film cooling distribution and cooling performance at x/D equal to 3, 13, 23 and 33. The results demonstrate that at a higher blowing ratio (BR=3.0 and 4.0) the interaction between the neighboring secondary airs leads to a full coverage film cooling effectiveness downstream of the fourth row, which is confirmed by the temperature field captured at x/D=33 and BR=4.0. The results also show that more cooling effectiveness is achieved at a shallow hole angle of ϕ=20 degrees, especially at higher blowing ratios in comparison with a baseline with a hole angle of ϕ=35 degrees. In line with this study, the researchers showed that the application of cooling holes with elevated injection angles enlarged the turbulence, and higher turbulence led to the cooling performance degradation (Sarkar et al. 1995). In addition, other researchers simulated a flat plate with cylindrical cooling holes to study the effects of injection angle on the effectiveness of film cooling (Nasir et al. 2001, Shine et al. 2013, Hale et al. 2000). They highlighted that lower stream-wise injection angles perform better to have a higher film cooling effectiveness.

Researchers presented experimental results of the study of temperature distribution inside a combustor simulator (Vakil et al. 2005). In this study, a real large scale of combustor was modelled. This model contained four different cooling panels with many cooling holes. Two rows of dilution jets could be seen in the second and third cooling panels. The first row had three dilution jets and the second one had two jets. While the first and second panels were flat, two other panels angled with an angle of 15.8 degrees. In this study, a real large scale of combustor was simulated and high momentum dilution jets and the coolant flow were injected into the main flow. The results indicated that high temperature gradient was developed upstream of the dilution holes. Other researchers re-simulated the Vakil and Thole's combustor (Kianpour et al. 2013, Kianpour et al. 2014). They offered various geometries of cooling holes. The temperatures near the wall and among the jets were higher for the baseline cooling whereas the central part of the jets was cooler in trenched cases.

By using a turbine vane cascade, the effects of shallow trenched holes (d=0.5D) were investigated to improve the performance of film cooling (Somawardhana et al. 2009). They measured the effectiveness of film cooling under blowing ratios ranging from BR=0.4 to 1.6. The findings indicated that upstream obstructions reduced the effectiveness by 50%. However, downstream obstructions increased the film cooling performance. The film cooling performance was slightly affected by a combination of obstructions near the upstream obstructions. Using a narrow trench, they dramatically modified the cooling performance and reduced the effects of surface roughness decrease. The results agreed with other findings (Harrison et al. 2009, Shuping. 2008). Also, Somawardhana and Bogard showed that higher film cooling effectiveness for the trenched holes which resulted from the net heat flux reduction was more than baseline case while the heat transfer coefficient was approximately constant for both cases. In contrast, researchers showed that trenching cooling holes increased heat transfer coefficient (Yiping et al. 2006). The results showed that the ratio of coolant momentum and the cooling effectiveness was reduced while at low blowing ratios the performance became better by traditional cooling holes (Ai et al. 2011).

Control volume technique and RNG k−ε turbulence model was used to investigate the flow and heat transfer behavior on flat plate film cooling from cone-shaped and round-shaped cooling holes (Zhang et al. 2006). They used RNG k−ε turbulent model to simulate the model and solve the Reynolds averaged Navier Stokes equation. The results showed that at the same blowing ratio, the film cooling effectiveness for the cone-shaped holes is better than round-shaped holes. For cone-shaped jets, the jet to cross flow blowing ratio reaches the optimum condition of 1.0 to yield the best film cooling effectiveness. The results indicated that a better thermal protection is attained at higher blowing ratios (Gao et al. 2009, Colban et al. 2008, Saumweber et al. 2003, Saumweber et al. 2013, Barigozzi et al. 2010).

In agreement with the study background, several authors have motivated the author to do this research. The endwall of the combustor can be damaged by the hot gases which flow inside a combustor simulator, and increasing the film cooling effectiveness above these surfaces is an important issue which has attracted less attention until now. In addition, most of the studies paid attention on the using of trenched holes at the leading edge of the turbine blades and in most of them the application of these holes at the endwall combustor was not considered. The alignment angle of the trenched cooling holes is a topic which was not considered in the past researches. This approach of cooling holes can also be utilized by engine designers at the fore side of the turbine vanes. Moreover, in order to measure the validity of the results, a comparison between the data gained from this study and the other project was carried out (Vakil et al. 2005, Stitzel et al. 2004).

2. Research methodology

In the present study, the combustor simulator applied was a 3-D representation of a Prat and Whitney gas turbine engine. As seen in Figure 1, the combustor was a three-dimensional container. The model's width, length and height were 111.7 cm, 156.9 cm and 99.1 cm respectively. The container converged from x/L=0.51 and the contraction angle was 15.8 degrees. The inlet and outlet cross-sectional area of the combustor simulator were 1.11m^2 and 0.62m^2, respectively.

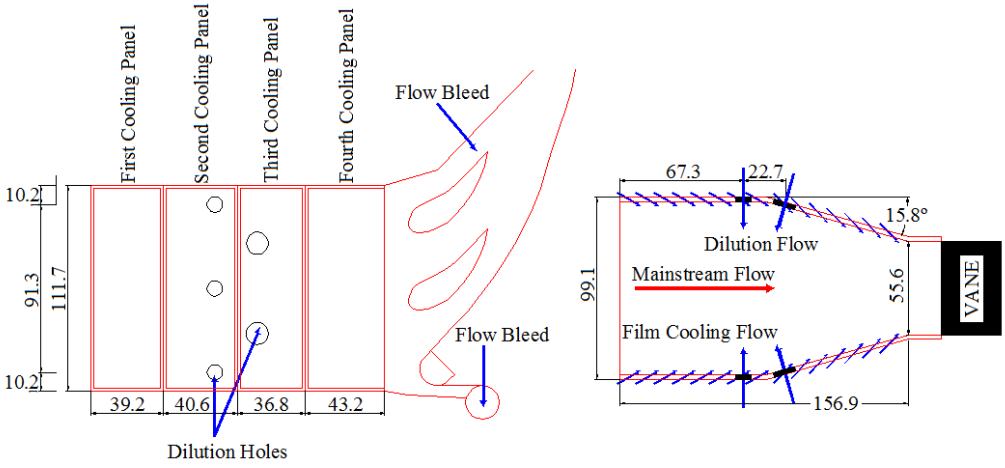

Fig. 1. Schematic view of the combustor simulator

The test section contained two symmetric surfaces on the top and bottom of the combustor but the fluid only flowed through bottom passage. The lengths of the cooling panels were 39cm, 41cm, 37 cm and 43 cm, respectively. In addition, the first two panels were flat and had constant sectional area. However, the last two panels were inclined at the contraction angle. The panels were 1.27cm thick, and due to the low thermal conductivity (k=0.037 W/mk) adiabatic surface temperature measurements were possible. Two different dilution rows were considered within the second and third panel of cooling panels. The dilution injected into the mainstream flowed vertically, while, the dilution hole in the third panel was angled at 15.8deg from the vertical axis. The first row of dilution jets included three holes and it was placed at 0.67m downstream of the combustor simulator inlet. These holes were 8.5cm in diameter. The second

row contained two dilution holes and was located at 0.23m downstream of the first row of the dilution holes' center. These holes diameter was 1.4 times more than the first one at 12.1cm. The centerline of the second row was staggered with respect to those of the first row. In the present research, the combustor simulator contained two arrangements of cooling holes. For the verification of findings, the first arrangement (baseline or case 1) was designed similar to the combustor modelled by (Vakil et al. 2005). The length of these cooling holes was 2.5cm and they drilled at an angle of 30deg from the horizontal surface. The film-cooling holes were 0.76cm in diameter.

Except the baseline case which is introduced, in order to investigate the effects of cooling holes trenching, row trenched holes with the alignment angle of 90 degrees with trench depth and width of 0.75D and 1.0D were considered. Furthermore, coolant blowing ratios were equal to BR=3.18. Therefore, the Cartesian coordinate system (x, y and z) was selected. The temperature of the coolant and dilution jets and mainstream flow was equal to 295.5 K and 332K respectively. Figure 2 shows the observation planes which are used to measure the film-cooling effectiveness distribution for baseline case and three different configurations of row trenched cooling holes. The observation planes of 0p, 1p, 2p, and 3p and 0s were placed in pitchwise and streamwise direction respectively. Plane 0p was located at x=35.1 cm. The distribution of film cooling momentum was computed along this panel. Plane 1p was located at the trailing edge of the first row of dilution jet. Plane 1p was developed from z=0 cm to z=10 cm and covered the whole width of the combustor simulator. It was applied to identify the effects of film cooling and dilution jets interaction, the horseshoe, half-wake and counter rotating vortexes effects. Plane 2p was placed at the trailing edge of the second row of dilution jets. It was placed at x⁄L=0.69 and was developed along the vertical axis. Plane 3p shown in Fig. 3 was applied to determine the behavior of outlet flow and the varying combustor temperature. At last, plane 0s was placed at the center of the first row of dilution jet at y=9.3 and extended from x=39.2 cm to x=78.45 cm. The importance of this plane was to identify the stream-wise behavior of the dilution jets first row.

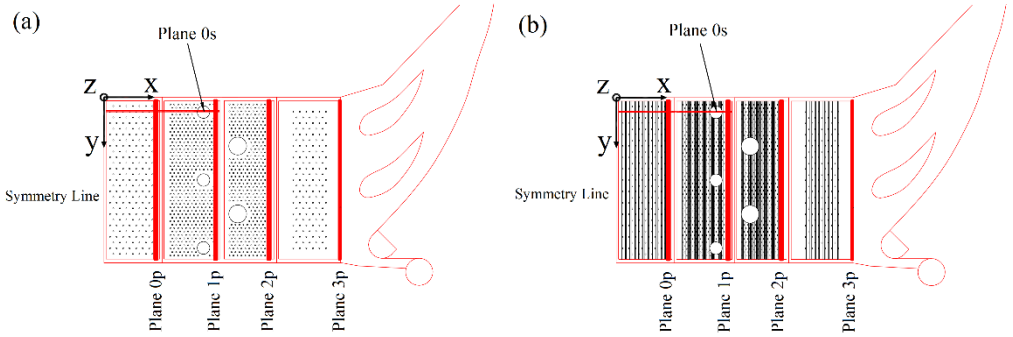

Fig. 2. Location of the observation planes: (a) Baseline; (b) Case 2

About 8×10^6 tetrahedral meshes were selected. The meshes were denser around the cooling and dilution holes as well as wall surfaces. According to the considered blowing ratio at the inlet of the control volume, the boundary condition of inlet mass flow was considered at the inlet. To limit the interaction region between the fluid and combustor wall, slip-less boundary condition and wall boundary condition were considered. In addition, two different boundary conditions of uniform flow and pressure outlet was selected at the inlet and outlet of the combustor, respectively. Totally, according to the symmetries of the Pratt and Whitney gas turbine engine combustor, symmetry boundary condition was used. Gambit package was

selected to mesh the combustor simulator and the model was analyzed by Fluent 6.2.26 software. The numerical method considered a transient, incompressible turbulent flow by means of the k–ε turbulent model of the Navier–Stokes equations expressed as follows:

Continuity equation

$$\frac{\partial}{\partial t}(\rho u_i)+\frac{\partial}{\partial x_j}=\rho\left(u_i u_j\right)=-\frac{\partial P}{\partial x_i}+\frac{\partial \tau_{ij}}{\partial x_i}+\rho \mathrm{g_i}+\vec{F_1} \tag{1}$$

Momentum equation

$$\frac{\partial}{\partial t}+\frac{\partial \rho}{\partial x}\frac{dx}{dt}+\frac{\partial \rho}{\partial y}\frac{dy}{dt}+\frac{\partial \rho}{\partial z}\frac{dz}{dt}=-\rho(\nabla.V) \tag{2}$$

Energy equation

$$\frac{\partial}{\partial t}(\rho E)+\frac{\partial}{\partial x_i}\left(u_i(\rho E+P)\right)=\frac{\partial x}{\partial x_i}\left[K_{eff}\frac{\partial T}{\partial x_i}-\sum_j h_j J_j+u_j\left(\tau_{ij}\right)_{erf}\right]+S_h \tag{3}$$

and k–ε equation

$$\frac{\partial}{\partial t}(\rho k)+\frac{\partial}{\partial x_i}(\rho k u_i)=\frac{\partial}{\partial x_j}\left[\left(\mu+\frac{\mu_t}{\sigma_k}\right)\frac{\partial k}{\partial x_j}\right]+P_k-\rho\varepsilon \tag{4}$$

$$\frac{\partial}{\partial t}(\rho \varepsilon)+\frac{\partial}{\partial x_i}(\rho \varepsilon u_i)=\frac{\partial}{\partial x_j}\left[\left(\mu+\frac{\mu_t}{\sigma_\varepsilon}\right)\frac{\partial \varepsilon}{\partial x_j}\right]+C_{1\varepsilon}\frac{\varepsilon}{k}P_k-C_{2\varepsilon}^{*}\rho\frac{\varepsilon^2}{k} \tag{5}$$

where P is static pressure, τ_{ij} is stress tensor, $\vec{F_1}$ is body force, ρ is the density, $\nabla.V$ is the velocity gradient, E is the energy, K_{eff} is effective conduction coefficient, S_h is the chemical reaction heat transfer and μ is the dynamic viscosity.

To investigate the convergence limit, the control volume mass residue has been estimated and the maximum value has been used. For this research, the criterion of convergence has chosen 10^{-4}. The following equation is to determine the effectiveness of film-cooling.

$$\eta=\frac{T-T_\infty}{T_c-T_\infty} \tag{6}$$

Here, T is the local temperature, and T_∞ and T_c are the temperatures of the mainstream and coolant.

3. Findings and discussion

The findings of the current research were compared with the experimental collected results and numerical findings gathered by other researchers (Vakil et al. 2005, Stitzel et al. 2004). The effectiveness of film-cooling was compared in plane 1p and 2p at y/W=0.4. The deviations between the results of current research and benchmarks were computed by the following equation:

$$\%Diff = \frac{\frac{\sum_{i=1}^{n} x_i - x_{i,benchmark}}{x_{i,benchmark}}}{n} \times 100 \quad (7)$$

For plane 1p, the deviation was equal to 9.76% compared to experimental measurements (Vakil et al. 2005) and 8.34% compared to CFD results (Stitzel et al. 2004). For observation plane of 2p, the deviation was 13.36% and 11.96% respectively (Figure 3).

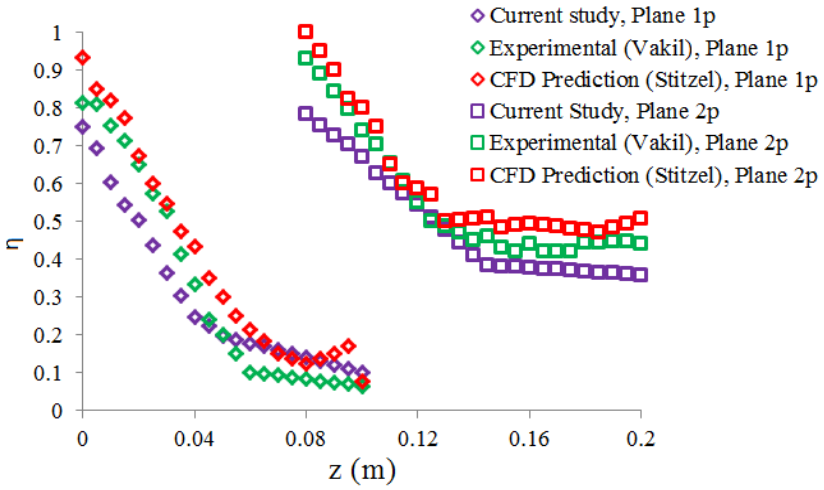

Fig. 3. The film cooling effectiveness comparison of planes 1p and 2p along y/W=0.4

Much of the film cooling effectiveness data in this study were collected on the assumption that symmetry could be applied within the combustor simulator. Fig. 4 shows a vertical film cooling effectiveness distribution taken at the intersection of panels 1p and 0s which extended over approximately 10% of the total inlet height at a high blowing ratio of 3.18.

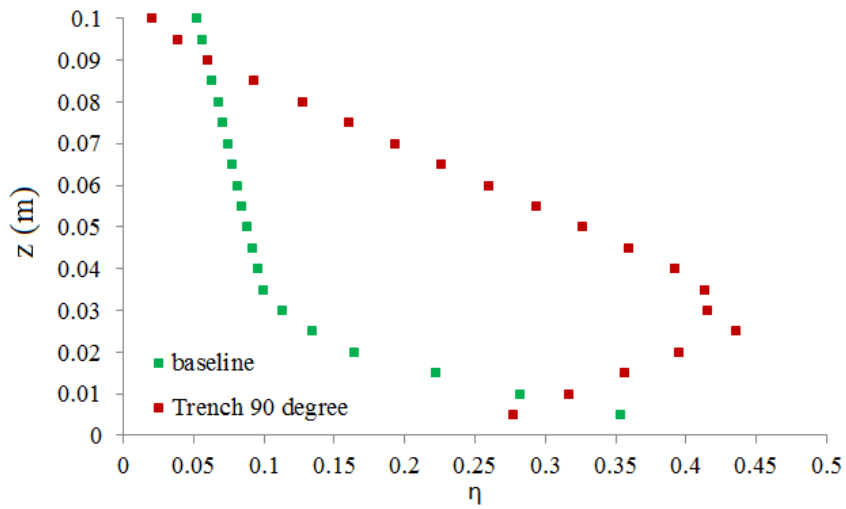

Fig. 4. Film cooling effectiveness at the intersection point of planes 1p and 0s

The trailing edge footprints of both dilution jets can be seen in the figure. According to Fig. 4, as the film cooling effectiveness reached η=0.353 adjacent the combustor end wall surface, the performance of baseline case was understandably more efficient than another one. As the vertical direction distance from the end wall surface grew larger, the cooling performance continuously reduced both for the baseline and the trenched holes with the alignment angle of 90 degrees.

Figure 5 shows the findings related to film cooling effectiveness of plane 1p at high blowing ratios of BR=3.18. Note that when film-cooling significantly increased, the dilution jet injection remained the same. Figure 5 shows slightly higher levels near the wall for the trenched case relative to the baseline. However, no major improvements in cooling were observed along the liner wall. It was just downstream of the dilution jet and near the corners that the thermal field contours indicated that the film-cooling were being entrained by the upward motion of the dilution jet. Moreover, the temperature was slightly higher (0<η<0.05) for the trenched holes with the alignment angle of 90 degrees at the position of 18cm<y<28cm and 38cm<y<50cm.

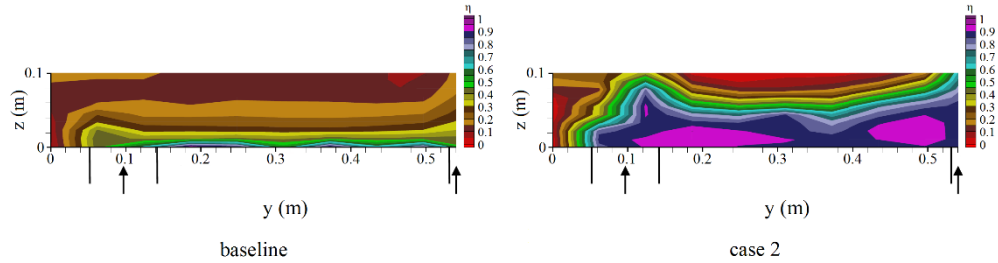

Fig. 5. Film cooling effectiveness for plane 1p

Figure 6 shows the contours of film cooling effectiveness in plane 2p at BR=3.18. The injection of a coolant into the mainstream is the basic difference between the obtained contours. Right at the trailing edge of the second row of dilution jets (10cm<y<50cm) and at higher blowing ratios, the trenched holes created a protective layer (0.9<η<1.0) on the critical surfaces which was more efficient than that of the baseline.

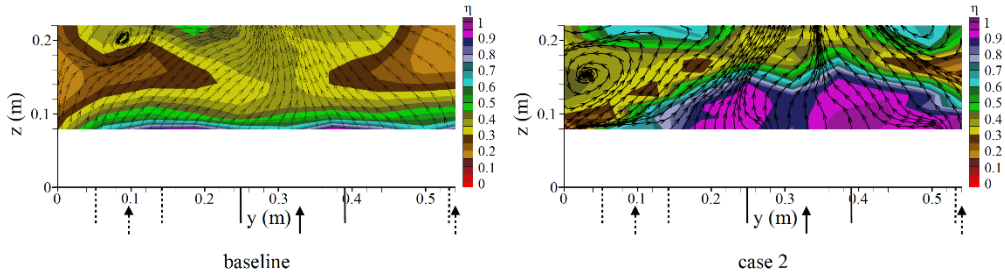

Fig. 6. Vectors of *v* and *w* overlaying temperature contours within plane 2p

A warmer area (0.15<η<0.20) expanded at the right (0cm<y<4cm) and left (48cm<y<52cm) sides of the thermal field contour. This figure shows the *v* and *w* velocity vectors superimposed on the top of the thermal field contours in plane 2p. It is visible for all arrangements that the coolant sweeps toward the second row of the dilution jet and accelerates near the combustor wall. However, vectors such as dominant vortical structures hardly show

any sign that might help with further mixing out the non-uniform temperature field. Fig. 7 shows the effects of hole geometries on a streamwise film cooling effectiveness distribution at BR=3.18.

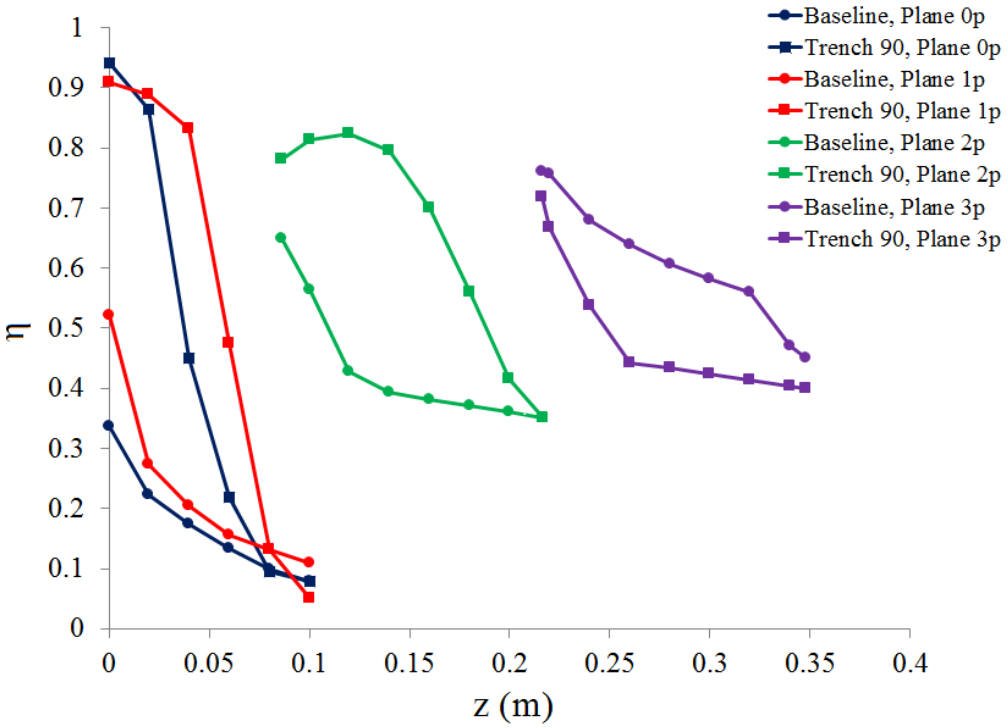

Fig. 7. Effect of trenching cooling holes on film cooling effectiveness distributions

The results show that the trenched holes with the alignment angle of 90 degrees performed the most effectively, especially in observation planes of 0p and 2p. This was 1.4 times as much the film cooling effectiveness of the baseline case. At this blowing ratio, the film cooling effectiveness of this kind of row trenched cooling holes has fluctuations at 0cm<z<2cm. The film exiting the trenches created a new boundary and enhanced heat transfer coefficients immediately downstream of the trench. In plane 3p, at BR=3.18 and due to the increase in the local interaction between the mainstream and jets, both cases of baseline and the trenched holes with the alignment angle of 90 degrees produced almost similar effectiveness, i.e. η=0.76 and η=0.718, respectively.

4. Conclusions

The commercial CFD code Fluent with RNG k-ε turbulence model was employed to analyze the effects of baseline case and row trenched cooling holes with different alignment angles under a blowing ratio of 3.18. Compared to the baseline method, in the trenched case, the coolant stayed closer to the end wall surface and did not allow the main entrainment. It also provided a significant lateral spreading and stronger coverage. Film cooling was also explored at high blowing ratios and the observation plane of 0p and 2p, using trenched holes with the alignment angle of 90 degrees. For plane 1p, at the trailing edge of the second cooling panel, the

row trenched holes with alignment angle of 90 degrees increased film cooling effectiveness by 75% which is much higher than baseline case. Comparisons between the data computationally predicted and those collected by others (Vakil et al. 2005, Stitzel et al. 2004) indicate the existence of similarities and differences. The predicted thermal field data indicated an under-predicted measurement for the current study as opposed to the experimental findings. An optimize design cooling holes will help to maximize the effectiveness of cooling along the combustor end wall surface and prevent premature wear in this area.

References

Abdullah K, Funazaki KI (2012). Effects of Blowing Ratio on Multiple Angle Film Cooling Holes. *AEROTECH IV Conference*, Kuala Lumpur, Malaysia.

Ai W, Laycock RG, Rappleye DS, Fletcher TH, Bons JP (2011). Effect of particle size and trench configuration on deposition from fine coal flyash near film cooling holes, *Energy & Fuels*, 25, 1066–1076.

Barigozzi G, Franchini G, Perdichizzi A, Ravelli S (2010). Film cooling of a contoured end wall nozzle vane through fan-shaped holes, *International Journal of Heat and Fluid Flow*, 31, 576–585.

Colban W, Thole KA, Haendler M (2008). A comparison of cylindrical and fan-shaped film-cooling holes on a vane end wall at low and high freestream turbulence levels, *Journal of Turbomachinery*, 130, 031007-1-031007-9.

Gao Z, Narzary D, Han JC (2009). Turbine Blade Platform Film Cooling With Typical Stator-Rotor Purge Flow and Discrete-Hole Film Cooling, *Journal of Turbomachinery*, 131, 041004-1-041004-11.

Hale CA, Plesniak MW, Ramadhyani S (2000). Film Cooling Effectiveness for Short Film Cooling Holes Fed by a Narrow Plenum, *Journal of Turbomachinery*, 122, 553-557.

Harrison KL, Dorrington JR, Dees JE, Bogard DG, Bunker RS (2009). Turbine Airfoil Net Heat Flux Reduction With Cylindrical Holes Embedded in a Transverse Trench, *Journal of Turbomachinery*, 131, 011012-1-011012-8.

Kianpour E, Sidik NAC, Wahid MA (2013). Cylindrical and Row Trenched Cooling Holes with Angle of 90º at Different Blowing Ratios, *CFD Letters*, 5, 165-173.

Kianpour E z, Sidik NAC (2014). Computational investigation of film cooling from cylindrical and row trenched cooling holes near the combustor endwall, *Case Studies in Thermal Engineering*, 4, 76-84.

Nasir H, Ekkad SV, Acharya S (2001). Effect of compound angle injection on flat surface film cooling with large streamwise injection angle, *Experimental Thermal and Fluid Science Journal*, 25, 23-29.

Salimi S, Fazeli A, Kianpour E (2014). Film Cooling Effectiveness Using Cylindrical and Compound Cooling Holes at the End Wall of Combustor Simulator, *Journal of Advanced Research in Fluid Mechanics and Thermal Sciences*, 1, 38-43.

Sarkar S, Bose TK (1995). Numerical simulation of a 2-D jet-crossflow interaction related to film cooling applications: Effects of blowing rate, injection angle and free-stream turbulence, *Sadhana*, 20, 915-935.

Saumweber C, Schulz A, Wittig S (2003). Free- Stream Turbulence Effects on Film Cooling With Shaped Holes, *Journal of Turbomachinery*, 125, 65-73.

Saumweber C, Schulz A (2012). Free-stream effects on the cooling performance of cylindrical and fan-shaped cooling holes, *Journal of Turbomachinery*, 134, 061007-1-061007-12.

Shine SR, Sunil Kumar S, Suresh BN (2013). Internal wall-jet film cooling with compound angle cylindrical holes, *Energy Conversion and Management*, 68, 54–62.

Shuping C (2008). *Film cooling enhancement with surface restructure*. PhD Theses. University of Pittsburgh. Pennsylvania.

Somawardhana RP, Bogard DG (2009). Effects of obstructions and surface roughness on film cooling effectiveness with and without a transverse trench, *Journal of Turbomachinery*, 131, 011010-1-011010-8.

Stitzel S, Thole KA (2004). Flow field computations of combustor-turbine interactions relevant to a gas turbine engine, *Journal of Turbomachinery*, 126, 122-129.

Vakil SS, Thole KA (2005). Flow and Thermal Field Measurements in a Combustor Simulator Relevant to a Gas Turbine Aero engine, *Journal of Engineering for Gas Turbines and Power*, 127, 257 -267.

Yiping L, Ekkad SV (2006). Predictions of film cooling from cylindrical holes embedded in trenches, *9th AIAA/ASME Joint Thermophysics and Heat Transfer Conference*, California, The United States of America.

Zhang XZ, Hassan I (2006). Numerical investigation of heat transfer on film cooling with shaped holes, *International Journal of Heat and Fluid Flow*, 16, 848-869.